



Contribution of whole genome sequencing in the molecular diagnosis of mosaic partial deletion of the *NF1* gene in neurofibromatosis type 1

Laurence Pacot^{1,2,3} · Valerie Pelletier⁴ · Albain Chansavang^{1,2} · Audrey Briand-Suleau^{1,2,3} · Cyril Burin des Roziers^{1,2,3} · Audrey Coustier¹ · Theodora Maillard¹ · Nicolas Vaucouleur¹ · Lucie Orhant¹ · Cécile Barbance¹ · Alban Lermine³ · Nadim Hamzaoui^{1,2,3} · Djihad Hadjadj² · Ingrid Laurendeau² · Laïla El Khattabi^{2,3,5} · Juliette Nectoux^{1,3} · Michel Vidaud^{2,3} · Béatrice Parfait^{1,2,3} · Hélène Dollfus^{4,6} · Eric Pasmant^{1,2,3} · Dominique Vidaud^{1,2,3}

Received: 11 June 2022 / Accepted: 19 July 2022

© The Author(s), under exclusive licence to Springer-Verlag GmbH Germany, part of Springer Nature 2022

Abstract

Neurofibromatosis type 1 (NF1) is an autosomal dominant disease with complete penetrance but highly variable expressivity. In most patients, Next Generation Sequencing (NGS) technologies allow the identification of a loss-of-function pathogenic variant in the *NF1* gene, a negative regulator of the RAS-MAPK pathway. We describe the 5-year diagnosis wandering of a patient with a clear NF1 clinical diagnosis, but no molecular diagnosis using standard molecular technologies. The patient presented with a typical NF1 phenotype but *NF1* targeted NGS, *NF1* transcript analysis, MLPA, and array comparative genomic hybridization failed to reveal a genetic aberration. After 5 years of unsuccessful investigations, trio WGS finally identified a de novo mosaic (VAF ~ 14%) 24.6 kb germline deletion encompassing the promoter and first exon of *NF1*. This case report illustrates the relevance of WGS to detect structural variants including copy number variants that would be missed by alternative approaches. The identification of the causal pathogenic variant allowed a tailored genetic counseling with a targeted non-invasive prenatal diagnosis by detecting the deletion in plasmatic cell-free DNA from the proband's pregnant partner. This report clearly highlights the need to make WGS a clinically accessible test, offering a tremendous opportunity to identify a molecular diagnosis for otherwise unsolved cases.

Introduction

Neurofibromatosis type 1 (NF1, [MIM: 162200]) is a fully penetrant autosomal disorder with an estimated incidence of 1 in 3500 live births. The main features of NF1 are multiple café-au-lait macules (CALMs), lentiginous macules, and a predisposition to benign and malignant tumors (Brems et al. 2009; Bergqvist et al. 2020). Other associated phenotypes include hyperreflective choroidal spots, short stature, macrocephaly, behavioral, and learning difficulties.

Traditionally, the identification of affected individuals has relied on clinical assessment and diagnosis according to standardized NIH criteria (Gutmann et al. 2017). While these criteria demonstrate a high positive predictive value to diagnose adult forms which commonly manifest as cutaneous and subcutaneous neurofibromas (NFs) that usually start developing in the teenage years, they perform less in the pediatric population, particularly in the absence of a family history (Kehrer-Sawatzki and Cooper 2022). Indeed, pathogenic variants could be found in only ~ 50% of children

✉ Eric Pasmant
eric.pasmant@aphp.fr

¹ Fédération de Génétique et Médecine Génomique, Hôpital Cochin, AP-HP, Centre-Université Paris Cité, 27 rue du Faubourg-Saint-Jacques, 75014 Paris, France

² Institut Cochin, Inserm U1016, CNRS UMR8104, Université Paris Cité, CARPEM, Paris, France

³ Plateforme SeqOIA, AP-HP, Paris, France

⁴ Medical Genetics Laboratory, INSERM U1112, Institute of Medical Genetics of Alsace, Strasbourg Medical School, University of Strasbourg, Strasbourg, France

⁵ Department of Cytogenetics, Hôpital Cochin, AP-HP, Centre-Université Paris Cité, Paris, France

⁶ Centre de Référence Pour les Affections Rares en Génétique Ophthalmologique, CARGO, Institut de Génétique Médicale d'Alsace, IGMA, Filiale SENS-GENE, Bâtiment du Centre de Recherche en Biomédecine Strasbourg (CRBS), Hôpitaux Universitaires de Strasbourg, Strasbourg, France

with ≥ 6 CALMs (Messiaen et al. 2009; Castellanos et al. 2020).

In more than 95% of cases, NF1 is caused by autosomal dominant loss-of-function variants in the *NF1* gene (Pasmant et al. 2012). *NF1* is located at 17q11.2 and two major isoforms of *NF1* transcript have been identified, containing 57 and 58 exons, respectively (isoform 1: NM_000267.3 and isoform 2: NM_001042492.3). While isoform 2 is the predominant transcript expressed in most tissue, isoform 1 is the most abundant form in the central nervous system (Perez-Becerril et al. 2021). The protein encoded by *NF1* is a GTPase activating protein (neurofibromin) that acts as a negative regulator of the RAS-mitogen-activated protein kinase (MAPK) signaling cascade (Ratner and Miller 2015). The *NF1* gene shows one of the highest mutation rates, with > 3700 different pathogenic variants referenced in public databases (Leiden Open Variation Database, LOVD and Human Gene Mutation Database, HGMD). The large spectrum of *NF1* pathogenic variants is distributed through the entire coding region and splice sites with no hotspot. Point mutations but also large deletions encompassing *NF1* and several neighboring genes were described (Sabbagh et al. 2013; Kehrer-Sawatzki et al. 2017; Pacot et al. 2021). More than 50% of *NF1* germline pathogenic variants arise de novo, resulting in a relatively high frequency of mosaicism. Patients with mosaic NF1 may more often develop mild NF1 phenotypes or manifestations limited to the affected area of the body with often unilateral manifestations. The presence of mosaic NF1 can complicate molecular diagnosis (with a low variant allele frequency of the pathogenic *NF1* variant) and specific criteria for mosaic NF1 have been defined, including neurofibroma analysis to help identify the causative *NF1* variation (Legius et al. 2021). It has been estimated that ~10% of sporadic NF1 patients have mosaic NF1 caused by postzygotic *NF1* mutations that are absent from, or present in, a very low proportion of blood lymphocytes (Messiaen et al. 2000).

Molecular analysis of the *NF1* gene is important in clinical practice to confirm a diagnosis, to differentiate from phenocopies, and to allow genetic counseling. Some of the NF1 clinical features are common to other diseases, such as Legius syndrome (OMIM#611431), an autosomal dominant disorder characterized by the presence of multiple CALMs, sometimes associated with skinfold freckling and macrocephaly or learning disabilities. Legius syndrome is caused by loss-of-function variants in the *SPRED1* gene, encoding a negative regulator of the RAS-MAPK (Brems et al. 2007, 2012; Pasmant et al. 2009a).

In this study, we describe a 5-year diagnosis wandering of a patient with a clear NF1 clinical diagnosis, but no molecular diagnosis following *NF1* characterization using NGS targeted sequencing, DNA microarray and transcript analysis. In the end, a whole-genome trio sequencing (WGS)

approach solved the enigma and allowed a tailored genetic counseling with a targeted non-invasive prenatal diagnosis (NIPD).

Materials and methods

Study samples and DNA extractions

Blood samples were collected on EDTA and PAXgene-Blood tubes (Becton Dickinson, Rungis, France). FFPE samples from two cutaneous neurofibromas were obtained from cutaneous surgical resections. DNA extraction was performed with the Maxwell 16 LEV Blood DNA and Maxwell 16 FFPE Tissue LEV DNA Kits (Promega, Charbonnières-Bains, France), respectively. RNA was extracted with the PAXgene RNA System (Qiagen, Courtaboeuf, France). Plasmatic cell-free DNA (cfDNA) was extracted using the QIAamp Circulating Nucleic Acid (Qiagen) from plasma collected in BCT Cell-Free DNA Collection Tube (Streck, Omaha, NE, USA).

Sanger sequencing

Polymerase chain reaction (PCR) was performed either on complementary DNA (cDNA) after reverse transcription of the NF1 transcript, or on DNA samples from blood samples. Amplified exons of the *NF1* gene (NM_001042492.3) were sequenced by Sanger sequencing using Big Dye Terminator chemistry and an ABI3100 Capillary Array Sequencer (Applied Biosystems). Primer sequences are available upon request. Sequences were aligned on the reference sequence with SeqScape analysis software v2.5 (Thermo Fisher Scientific).

Targeted next-generation sequencing

Experiments were performed at the NGS facility of Cochin Hospital, Paris (*Assistance Publique- Hôpitaux de Paris*, AP-HP, France), as previously described (Pasmant et al. 2015; Louvrier et al. 2018). *NF1* and *SPRED1* exons and flanking intronic regions were amplified with a custom-made panel (Thermo Fisher Scientific) and sequenced on NextSeq500 (Illumina). Sequence alignment, variant calling, and variant annotation were performed using MOABI Leaves pipeline (AP-HP). The copy number variations (CNVs) were assessed using the number of reads for each amplicon of each sample. Read number for each *NF1* and *SPRED1* amplicon was normalized by dividing each amplicon read number by the total of amplicon read numbers of a control gene from the same sample, each gene serving as a control for the CNV analysis of the other. Normalised read numbers obtained for each amplicon of a sample were

then divided by the average normalised read number of control samples for the corresponding amplicon. Copy number ratios <0.7 and >1.3 were considered deleted and duplicated, respectively.

Whole genome sequencing (WGS)

The trio WGS was performed at the SeqOIA laboratory (<https://laboratoire-seqoia.fr/>). The library was prepared using the NEB Next Ultra II End repair/A-tailing DNA Library Prep Kit (New England Biolab, Ipswich, MA, USA) and sequenced in paired ends (2×150 bp) using an Illumina Novaseq6000 platform. The reads were aligned to the reference human genome (GRCh38.92) using the BWA-MEM 0.7.15 software package. The GATK haplotype caller (v4.1.7.0; Broad Institute) was used to call the SNVs, and CNVnator (v0.4.1; Mark B, Yale University) was used for CNV calling. ClinSV (Minoche et al. 2021), a WGS-based bio-informatic framework that combined different methods based on read depth, was used to annotate and prioritize structural variants, including CNVs. The resulting variants were then annotated with AnnotSVv2.5.1 in an in-house developed workflow (SeqOIA-IT platform).

Multiplex ligation-dependent probe amplification (MLPA) analysis

Single and multi-exon deletion/duplication screening was performed with MLPA analysis using the SALSA MLPA P081/P082 NF1 and P295 SPRED1 kits (MRC Holland, Amsterdam, Netherlands), as previously described (Sabagh et al. 2013; Pasmant et al. 2015; Pacot et al. 2021). Briefly, four control samples and each NF1 patient sample (each containing 100 ng of genomic DNA) were used for overnight hybridization with the probe mixes. After ligation and amplification were performed with FAM-labelled primers, PCR products were analyzed on an ABI Prism 3130 automatic DNA sequencer (Life Technologies).

Molecular cytogenetic analyses

Chromosomal analysis was carried out using an oligonucleotide array with a probe spacing of 50 kb on average providing a mean resolution of 250 Kb (SurePrint G3 ISCA v2 CGH 8×60 K Microarrays, Agilent) (Pasmant et al. 2009b). Analysis and graphical representation of the data were performed using CytoGenomics v5.1 and Cartagenia software.

Microsatellite typing

Familial segregation of four *NF1* intragenic polymorphic microsatellites (D17S1307, D17S2163, D17S1166 and GDB:270136) and three *NF1* extragenic polymorphic

microsatellites (D17S841, D17S1800, and D17S798) was used for CNV analysis (Pasmant et al. 2008). The primer oligonucleotide sequences are available upon request. DNA samples were diluted at a concentration of 10 ng/mL and amplified using dedicated primers and the Taq GOLD polymerase (Thermo Fisher Scientific). The GS-500LIZ (Thermo Fisher Scientific) marker was used for detection. Maternity and paternity were assessed using a PowerPlex 16 HS System (Promega) according to the manufacturer's instructions. Scaling was controlled with 2800 M Control DNA (Promega). Microsatellites analysis was performed on an ABI Prism 3130 automatic DNA sequencer (Thermo Fisher Scientific, Courtaboeuf, France). The results were analyzed with the GeneMapper v.4.0 software package (Thermo Fisher Scientific).

Digital droplet PCR

Nine microliters of the cfDNA were mixed with 10 μ L of ddPCR Super-mix for Probes (Biorad, CA, USA) and 1 μ L of each PCR primers/probes duplex. Droplets were generated in the QX200 Droplet generator (Biorad). Fluorescence data were converted into concentrations according to Poisson distribution statistical analysis using the QuantaSoft Analysis Pro software v1.0.596 (Biorad). Fetal fraction was estimated using the *RASSF1A/ACTB* assay, as previously described (Huby et al. 2021). ddPCR amplification of the promoter region of the *RASSF1A* gene, known to be differentially methylated between the mother DNA (lymphocytes) and the fetal DNA (placenta), was used to assess the presence of fetal DNA. Co-amplification of *RASSF1A* and *ACTB* was performed, before and after BstUI digestion (New England Biolabs, Beverly, MA, USA). In the absence of positive droplets for *ACTB* after digestion, fetal fraction was calculated as follows: $[\text{RASSF1A}]_{\text{postdigestion}}/[\text{RASSF1A}]_{\text{predigestion}}$ (four replicates).

Variants nomenclature and interpretation

Variants were named at the coding DNA, RNA, and protein levels according to the Human Genome Variation Society (HGVS) recommendations. An assessment of variants' pathogenicity was performed according to the *American College of Medical Genetics and Genomics and the Association for Molecular Pathology (ACMG-AMP)* guidelines. Assessment of variants implication was mainly performed based on population databases (gnomAD v2.1.1), variant databases (ClinVar v20220205 and LOVD-NF1), and predictions softwares. In silico predictions of the effect of the variant were performed with CADD (Rentzsch et al. 2021), SPiP (Raphaël Leman et al. 2022), dbScSNV (Jian et al. 2014), PROVEAN (Choi et al. 2012), Human Splice Finder (HSF) (Desmet

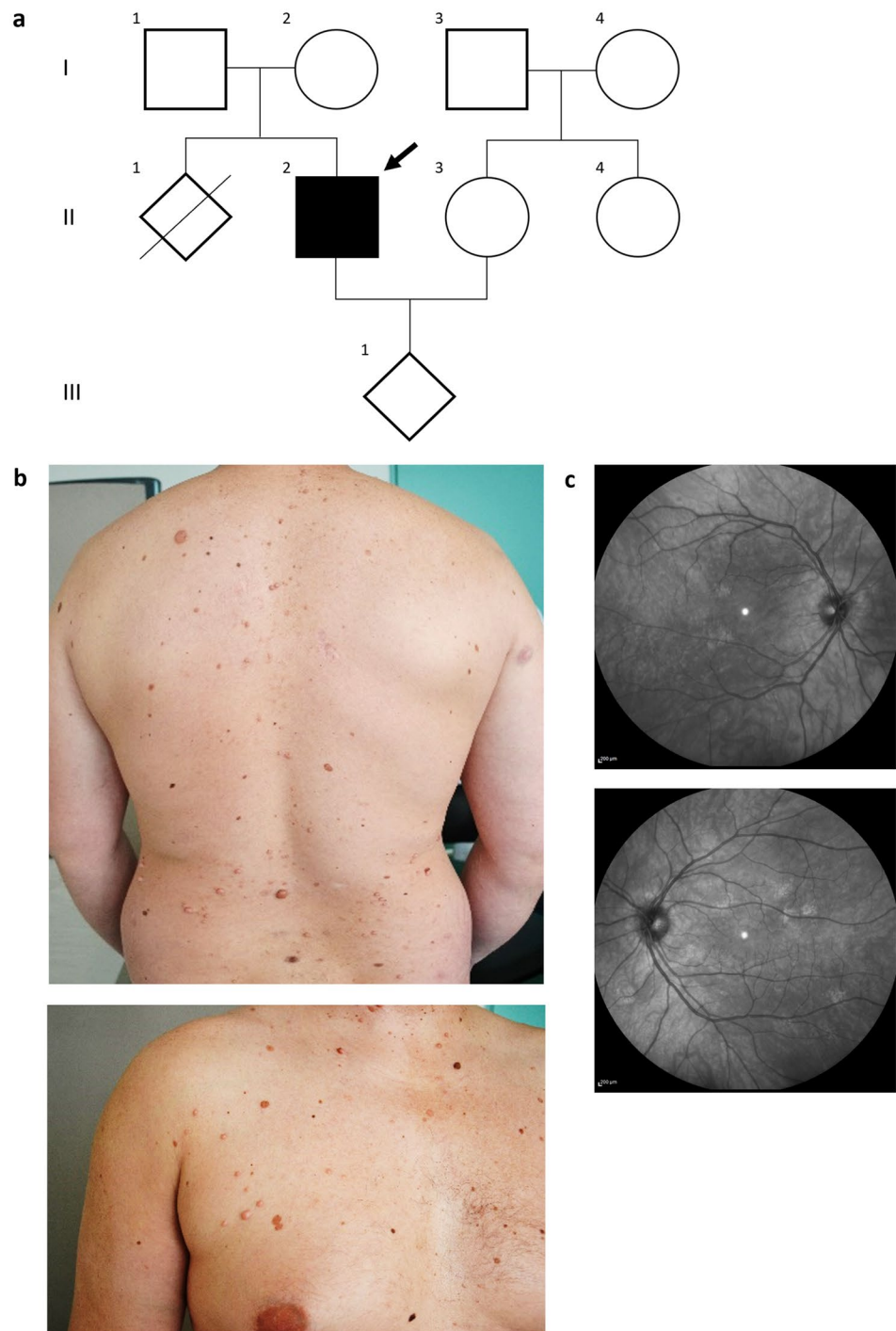
et al. 2009), and MaxEntScan (Yeo and Burge 2004). *NF1* variants are reported according to the reference sequence NM_001042492.3 (ENST00000358273.9; NF1-202).

Results and discussion

Patient's phenotype

In 2015, the proband, a 31-year-old male, first presented with cutaneous neurofibromas (NFs), Lisch nodules, and >6 CALMs mainly located in the trunk area (Fig. 1). Magnetic

Fig. 1 Family pedigree and clinical photographs. **a** Family pedigree. The patient presenting with NF1 phenotype is shown in black. **b** Clinical phenotype of the index case with multiple café-au-lait spots and cutaneous neurofibromas. **c** Near-infrared imaging of the index case's right (upper image) and left (bottom image) eyes showing choroidal abnormalities: bright patchy regions typical of NF1



resonance imaging of the brain showed eight hyperintense T2-weighted lesions (unidentified bright objects) in the right subtentorial white matter structure. Near-infrared reflectance imaging showed choroidal abnormalities (bright patchy regions) typical of NF1 (Yasunari et al. 2000) (Fig. 1c). No cardiovascular abnormality, learning disability or skeletal malformation was identified, except from a mild scoliosis. No malignant tumor nor optic pathway glioma was evidenced with clinical and radiological explorations. The proband was the first child of healthy nonconsanguineous parents. The proband was clinically diagnosed with NF1 as he had numerous cutaneous NFs, CALMs, and bilateral Lisch nodules (Legius et al. 2021).

Initial molecular analyses

In 2016, a targeted NGS panel in the proband's germline DNA identified an *NF1* heterozygous (estimated variant allele frequency, VAF ~ 49%, 363/745 reads) c.5943+65 T>C intronic variant. This variant was found neither in population databases (gnomAD) nor in ClinVar or LOVD databases. In silico analysis of the *NF1* c.5943+65T>C variant (intron 40) did not predict an alteration of the splice site. The c.5943+65T>C *NF1* variant was, therefore, classified as of uncertain significance (pathogenic criteria were not met), according to ACMG-AMP criteria (Richards et al. 2015) with the following criteria: (i) absence of the variant in the population databases (pathogenic moderate criterion: PM2), (ii) patient's phenotype highly specific for a gene (pathogenic supporting criterion: PP4), and (iii) multiple lines of computational evidence suggest no impact on *NF1* splicing (benign supporting criterion: BP4).

To reclassify this variant, additional molecular analyses were performed. Sanger sequencing in the proband's parents identified the c.5943+65 T>C variant in his unaffected mother's blood DNA; both maternity and paternity were confirmed using the familial segregation of 15 short tandem repeat (STR) markers. Clinical examination of the mother and father showed no signs of NF1. As NF1 is a simply determined Mendelian disorder with complete penetrance, the identification of the variation in the unaffected mother of the index case supported the benign status of the variant. In 2018, a transcript study of *NF1* was performed on total RNAs extracted from a blood sample of the proband (PAXgene tube). This study did not allow the identification of any transcript alteration or splicing defect, confirming in silico predictions. Transcript analysis confirmed the biallelic expression of *NF1*, with the presence of 2 polymorphisms (rs1801052 and rs2285892). These observations also argued against the pathogenicity of the variant. Based on these additional analyses, the c.5943+65T>C *NF1* variant was finally reclassified as benign, according to the following

ACMG-AMP criteria: (i) observation in control inconsistent with disease penetrance (benign strong criterion: BS2), (ii) well-established functional studies showed no deleterious effect (BS3), and (iii) multiple lines of computational evidence suggested no impact on splicing (benign supporting criterion: BP4).

Complementary analyses on blood and neurofibromas

Further analyses were conducted to identify a genetic alteration that would have been missed by previous analyses. Analysis of four *NF1* intragenic and three extragenic microsatellite markers did not reveal any alteration suggestive of a copy number variation (CNV). *NF1* and *SPRED1* targeted MLPA, standard karyotype, and 250 k resolution array comparative genomic hybridization (aCGH) did not reveal any alteration. Given the failure to identify a constitutional event, molecular genetic analyses were carried out on DNA extracted from two different cutaneous NFs resected from the proband. In 2017, targeted *NF1* and *SPRED1* NGS identified two different heterozygous somatic pathogenic variants in the *NF1* gene: (i) c.2299G>T p.(Glu767*) (VAF ~ 19%, 414/2124 reads) in the first cutaneous neurofibroma and (ii) c.5329C>T p.(Gln1777*) (VAF ~ 12%, 295/2374 reads) in the second neurofibroma. The identification of two distinct *NF1* tumoral second hits in the two different neurofibromas, as well as the typical NF1 phenotype of the patient, suggested the existence of a pathogenic constitutional *NF1* variant which was missed by our former investigations.

Whole-genome sequencing

In 2021, taking advantage of the *French Plan for Genomic Medicine 2025*, a whole-genome sequencing (WGS) approach was proposed. A trio WGS, including the constitutional DNA sample from the proband and his parents was performed. The WGS metrics for the index case were as follows: Bases \geq Q30 = 107 Gb; 96.3% of genome \geq 15X reads with mapq > 20; 90% of callability (WG); and mean depth = 35.6X. A de novo mosaic (VAF ~ 14%, evidenced on 6 discordant paired-end or split reads and absent in the parents' DNAs) germline 24.6 kb deletion encompassing part of the promoter and the first exon of *NF1* (Fig. 2a) was identified: NC_000017.11:g.31089153_31113754=/del (GRCh38.p13). The variant was classified as pathogenic, according to ACMG-AMP criteria with the following criteria: (i) predicted null variant in a gene where loss-of-function is a known mechanism of disease (PVS1), (ii) de novo variant (both maternity and paternity confirmed) in a patient with the disease and no family history (PS2), (iii) absence of the variant in population databases (PM2), and (iv) patient's phenotype highly specific for the gene (PP4). The

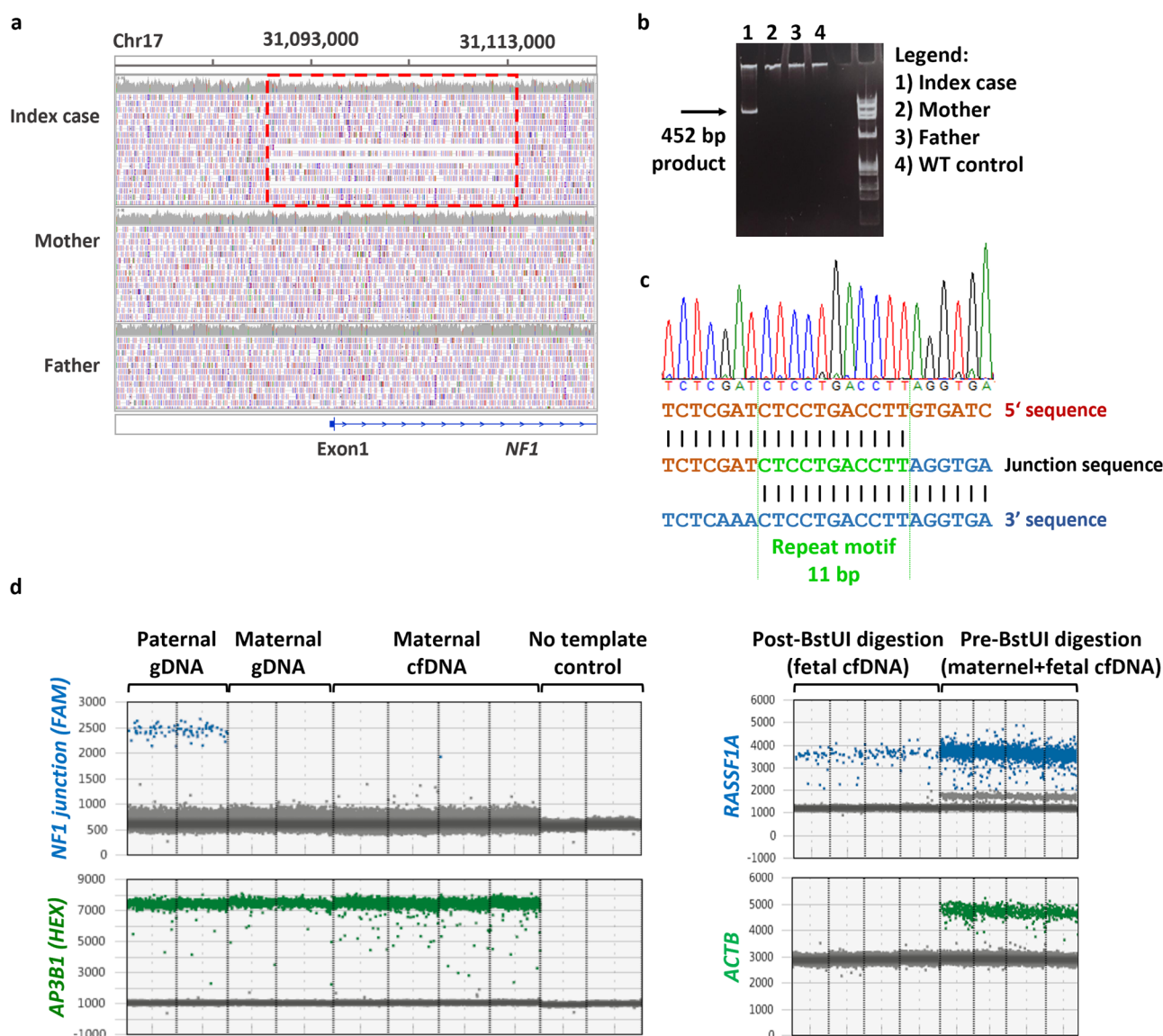


Fig. 2 Molecular characterization of the deletion. **a** Read alignment at the deletion locus of chromosome 17. Read alignments and deletion were visualized using the Integrative Genomics Viewer (IGV) (Robinson et al. 2011). The red dashed box indicates the deleted region. **b** PCR results and **c** Sanger sequencing electropherogram of the deletion junction detected only for the index case but not for his parents nor the control, with primers (U1: 5'-TGGAGTCCTTGCCAG AATGT-3' and L1: 5'-ATCTGTATAAAGGCTGAGTGGTCAA-3'). An 11 bp homologous sequence (green shade) is present at both breakpoints of the deletion. **d** NIPD using a ddPCR assay excluding the paternal *NF1* pathogenic deletion, NC_000017.11:g.31089144_31113701del. On the left panel: one-dimensional scatter plots for NC_000017.11:g.31089144_31113701del *NF1* assay, showing the absence

of the deletion (absence of breakpoint fragment amplification) in the merged replicates in maternal cfDNA. Parental genomic DNAs (gDNA) are tested simultaneously in plasma cell-free DNA (cfDNA), as positive and negative controls, respectively. Blue droplets are positive for the deleted allele (breakpoint fragment amplification), green droplets are positive for *AP3B1* (control gene) WT allele, grey droplets are negative droplets; (right panel) one-dimensional scatter plots for *RASSF1A/ACTB* assay before and after BstUI digestion. Presence of fetal DNA in maternal cfDNA is confirmed by the detection of *RASSF1A*-positive blue droplets after BstUI digestion. The fetal fraction, calculated by dividing the digested-*RASSF1A* droplet count by the undigested-*RASSF1A* droplet count, was evaluated at 6%

expected consequence of this variant was a complete loss of *NF1* expression. Mutations in the *NF1* promoter/5'UTR are not frequently described. Only one pathogenic deletion in the *NF1* promoter was reported in the LOVD database (c.-915_-262del, DB-ID NF1_002259). Two variants in the

NF1 5'UTR were previously reported as likely pathogenic based on conservation and de novo occurrence or co-segregation with the disease: c.-272G>A and c.-273A>C (Evans et al. 2016).

This large intragenic *NF1* deletion was consistent with the classical NF1 phenotype observed in the patient. The lack of identification of this mosaic deletion by previous techniques might be explained by (i) the low rate of mosaicism (VAF estimated at 14%), combined with (ii) the amplification heterogeneity of the first exon of *NF1* caused by its GC-rich sequence. This second point may also explain the scarcity of reported pathogenic variants in the promoter region of the *NF1* gene, together with the difficulty of interpreting such variants (Horan et al. 2004). The homogeneity of coverage of the WGS approach, as well as the sequencing of non-coding regions (*NF1* promoter and first intron) allowed the deletion detection.

To confirm its precise size and breakpoints, we then characterized the deletion breakpoints with a dedicated breakpoint PCR and Sanger sequencing: only samples from the propositus yielded a specific 452 bp fragment (Fig. 2b, c). The deletion was 24,602 bp long and breakpoints were located within an 11 bp repeat motif in two short interspersed nuclear element Alu sequences (proximal breakpoint: AluY and distal breakpoint: AluSx), suggesting a homologous recombination mechanism. Digital droplet PCR (ddPCR) specific to the junction fragment estimated the deletion VAF at ~ 10% in the blood sample and ~ 15% and ~ 13% in the two cutaneous NFs. This low VAF was nevertheless compatible with a typical NF1 phenotype. Some mosaic forms of NF1 can result in a specific form of the disease: segmental NF1 is defined by a limited condition of a quadrant or sector, with pigmentation abnormalities following the lines of Blaschko that become partially visible. Other mosaïcisms can show typical NF1 presentation. These different NF1 mosaic phenotypes may reflect the embryonic timing and, accordingly, the neural crest-derived cell types involved in the post-zygotic *NF1* pathogenic variant (Maertens et al. 2007; Biesecker and Spinner 2013).

Genetic counselling and prenatal diagnosis

After 5 years of unsuccessful investigations, WGS finally allowed the identification of an *NF1* intragenic mosaic deletion that had not been identified by targeted routine molecular techniques. A recent broad international effort initiated to revise the criteria for NF1 diagnosis led to the incorporation of genetic testing into the revised NF1 diagnostic criteria, with specific diagnostic criteria for mosaic NF1 (Legius et al. 2021). Hence, it can be expected that genetic testing will become standard-of-care for a definite diagnosis which is becoming increasingly relevant with constantly improving strategies for clinical management. Identification of the individual *NF1* pathogenic variant allowed to propose genetic counselling to the index case and his wife. NF1 follows an autosomal dominant transmission mode with a 50% risk to inherit the pathogenic variant in the case of a constitutional

alteration. The couple received and understood a detailed information on the clinical features of NF1 from clinicians. The risk of transmission and the high clinical variable expressivity of NF1 were discussed. The couple did not want to take the risk of transmitting the disease because of its potential severe complications, the uncertainty of the disease course, and the extensive medical follow-up. After several discussions, the multidisciplinary prenatal diagnosis center authorized a prenatal test, considering the patient's request and the strong probability and severity of the disease.

The presence of fetal DNA in pregnant women plasma allows NIPD for severe monogenic diseases through maternal blood collection, which prevents from fetal loss risk due to invasive procedures. In maternal plasma, cell-free fetal DNA is mixed with a large proportion of maternal cell-free DNA (cfDNA) that predominantly originates from the mother's blood cells. Thus, one way to reliably detect fetal DNA in maternal plasma is to analyze nucleotide sequences that are specific to the fetus and distinguishable from the maternal DNA, such as paternally inherited variants. Hypermethylated *RASSF1A* promoter was used as a fetal marker to confirm the presence of cell-free fetal DNA. Hypomethylated maternal sequences were digested using methylation-sensitive restriction enzymes, leaving hypermethylated fetal sequences detectable (Fig. 2d). Several ddPCR assays have been developed for NIPD application, such as sex determination, fetal RHD genotyping, aneuploidy detection, and monogenic disorders (Gruber et al. 2018; El Khattabi et al. 2019; Huby et al. 2021). A non-invasive method was chosen because it avoids the 0.5% miscarriage risk associated with the current invasive procedure (Salomon et al. 2019) and it only requires a blood sample. ddPCR allows precise quantification of rare events and was performed as a personalized medicine service with a specific design of primers and probes as well as assay qualification for the *NF1* deletion breakpoints. As the proband's wife did not carry the *NF1* pathogenic variant, an exclusion diagnosis by a dedicated breakpoint ddPCR could be performed directly on cfDNA extracted from her plasma. NIPD was performed at 10 weeks and 4 days of amenorrhea, based on the detection of the father's *NF1* pathogenic deletion in maternal blood cell-free DNA, using ddPCR of the breakpoint fragment. The variant was not detected in the cfDNA while the presence of fetal DNA was confirmed: the *NF1* paternal pathogenic variant was therefore excluded in the fetus (Fig. 2d). The result was confirmed at 12 weeks and 4 days of amenorrhea and the pregnancy was completed.

Conclusion

In this study, we described a 5-year diagnostic wandering, resolved by a trio WGS approach (Online Fig. S1). The typical NF1 clinical features coupled with tumoral *NF1* second

hits provided a compelling argument for an *NF1* alteration in the proband. Tumor tissue analysis to identify the constitutional variant is the most relevant in mosaic cases. The culture of primary cells from NF1-associated lesions (Schwann cells from neurofibromas or melanocytes from CALMs) may also improve the detection of mosaic variants by enriching the samples with variant-carrying cells (Maertens et al. 2007). This case report illustrates the relevance of WGS to detect CNVs and other structural variants that would be missed by targeted NGS, genotyping or aCGH. WGS outperforms microarrays for the detection of clinically relevant CNVs, arguing for its use as a single assay for genetic variation detection (Trost et al. 2018; Collins et al. 2020). In the present case, the mosaic deletion of a GC-rich region was not previously detected by standard approaches. The identification of a causal pathogenic variant by WGS allowed a tailored genetic counseling with a targeted NIPD approach. This clearly highlights the need to make WGS a clinically accessible test, offering a tremendous opportunity to identify a molecular diagnosis for otherwise unresolved cases (100,000 Genomes Project Pilot Investigators et al. 2021).

Supplementary Information The online version contains supplementary material available at <https://doi.org/10.1007/s00439-022-02476-3>.

Acknowledgements We thank all participants and their referring physicians.

Author contributions All authors made substantial contributions to the work, as follows: V.P. and H.D. made substantial contributions to primary clinical data collection; M.V. supervised and performed the whole-genome analysis and variant validation; A.L., A.B-S., C.B.d.R. coordinated the whole-genome alignment, variant calling and variant interpretation; A.C., T.M., N.V., L.O., I.L., and C.B. made substantial contributions to molecular genetic experiments; N.H., D.H., B.P., L.E.K., J.N., and A.C. performed the genetic analyses; E.P., D.V., and L.P. substantially contributed to study concept and design and manuscript writing; analysis and interpretation of data as well as drafting of the manuscript; All authors provided critical review of the paper, have approved the submission, and accept responsibility for their contribution.

Funding No specific funding was obtained for this study.

Availability of data and materials The data that support the findings of this study are available from the corresponding author upon reasonable request.

Declarations

Conflict of interest The authors declare that they have no competing interests.

Ethical approval The study is in line with the current French legislation on genetic studies.

Consent for publication Patient and his parents gave their written informed consent for the use of their clinical and genetic data in the context of research.

References

- 100,000 Genomes Project Pilot Investigators, Smedley D, Smith KR, et al (2021) 100,000 Genomes Pilot on Rare-Disease Diagnosis in Health Care—Preliminary Report. *N Engl J Med* 385:1868–1880. <https://doi.org/10.1056/NEJMoa2035790>
- Bergqvist C, Servy A, Valeyrie-Allanore L et al (2020) Neurofibromatosis 1 French national guidelines based on an extensive literature review since 1966. *Orphanet J Rare Dis* 15:37. <https://doi.org/10.1186/s13023-020-1310-3>
- Biesecker LG, Spinner NB (2013) A genomic view of mosaicism and human disease. *Nat Rev Genet* 14:307–320. <https://doi.org/10.1038/nrg3424>
- Brems H, Beert E, de Ravel T, Legius E (2009) Mechanisms in the pathogenesis of malignant tumours in neurofibromatosis type 1. *Lancet Oncol* 10:508–515. [https://doi.org/10.1016/S1470-2045\(09\)70033-6](https://doi.org/10.1016/S1470-2045(09)70033-6)
- Brems H, Chmara M, Sahbatou M et al (2007) Germline loss-of-function mutations in SPRED1 cause a neurofibromatosis 1-like phenotype. *Nat Genet* 39:1120–1126. <https://doi.org/10.1038/ng2113>
- Brems H, Pasmant E, Van Minkelen R et al (2012) Review and update of SPRED1 mutations causing Legius syndrome. *Hum Mutat* 33:1538–1546. <https://doi.org/10.1002/humu.22152>
- Castellanos E, Rosas I, Negro A et al (2020) Mutational spectrum by phenotype: panel-based NGS testing of patients with clinical suspicion of RASopathy and children with multiple café-au-lait macules. *Clin Genet* 97:264–275. <https://doi.org/10.1111/cge.13649>
- Choi Y, Sims GE, Murphy S et al (2012) Predicting the functional effect of amino acid substitutions and indels. *PLoS ONE* 7:e46688. <https://doi.org/10.1371/journal.pone.0046688>
- Collins RL, Brand H, Karczewski KJ et al (2020) A structural variation reference for medical and population genetics. *Nature* 581:444–451. <https://doi.org/10.1038/s41586-020-2287-8>
- Desmet F-O, Hamroun D, Lalonde M et al (2009) Human splicing finder: an online bioinformatics tool to predict splicing signals. *Nucleic Acids Res* 37:e67. <https://doi.org/10.1093/nar/gkp215>
- El Khattabi LA, Brun S, Gueguen P et al (2019) Performance of semiconductor sequencing platform for non-invasive prenatal genetic screening for fetal aneuploidy: results from a multi-center prospective cohort study in a clinical setting. *Ultrasound Obstet Gynecol* 54:246–254. <https://doi.org/10.1002/uog.20112>
- Evans DG, Bowers N, Burkitt-Wright E et al (2016) Comprehensive RNA analysis of the NF1 gene in classically affected NF1 affected individuals meeting NIH criteria has high sensitivity and mutation negative testing is reassuring in isolated cases with pigmentary features only. *EBioMedicine* 7:212–220. <https://doi.org/10.1016/j.ebiom.2016.04.005>
- Gruber A, Pacault M, El Khattabi LA et al (2018) Non-invasive prenatal diagnosis of paternally inherited disorders from maternal plasma: detection of NF1 and CFTR mutations using droplet digital PCR. *Clin Chem Lab Med* 56:728–738. <https://doi.org/10.1515/cclm-2017-0689>
- Gutmann DH, Ferner RE, Listernick RH et al (2017) Neurofibromatosis type 1. *Nat Rev Dis Primers* 3:17004. <https://doi.org/10.1038/nrdp.2017.4>
- Horan MP, Osborn M, Cooper DN, Upadhyaya M (2004) Functional analysis of polymorphic variation within the promoter and 5' untranslated region of the neurofibromatosis type 1 (NF1) gene.

- Am J Med Genet A 131:227–231. <https://doi.org/10.1002/ajmg.a.30358>
- Huby T, Le Guillou E, Burin des Roziers C et al (2021) Non-invasive prenatal diagnosis of a paternally inherited MEN1 pathogenic splicing variant. *J Clin Endocrinol Metab*. <https://doi.org/10.1210/clinem/dgab894>
- Jian X, Boerwinkle E, Liu X (2014) In silico prediction of splice-altering single nucleotide variants in the human genome. *Nucleic Acids Res* 42:13534–13544. <https://doi.org/10.1093/nar/gku1206>
- Kehrer-Sawatzki H, Cooper DN (2022) Challenges in the diagnosis of neurofibromatosis type 1 (NF1) in young children facilitated by means of revised diagnostic criteria including genetic testing for pathogenic NF1 gene variants. *Hum Genet* 141:177–191. <https://doi.org/10.1007/s00439-021-02410-z>
- Kehrer-Sawatzki H, Mautner V-F, Cooper DN (2017) Emerging genotype–phenotype relationships in patients with large NF1 deletions. *Hum Genet* 136:349–376. <https://doi.org/10.1007/s00439-017-1766-y>
- Legius E, Messiaen L, Wolkenstein P et al (2021) Revised diagnostic criteria for neurofibromatosis type 1 and Legius syndrome: an international consensus recommendation. *Genet Med* 23:1506–1513. <https://doi.org/10.1038/s41436-021-01170-5>
- Louvrier C, Pasmant E, Briand-Suleau A et al (2018) Targeted next-generation sequencing for differential diagnosis of neurofibromatosis type 2, schwannomatosis, and meningiomatosis. *Neuro Oncol* 20:917–929. <https://doi.org/10.1093/neuonc/nyy009>
- Maertens O, De Schepper S, Vandensompele J et al (2007) Molecular dissection of isolated disease features in mosaic neurofibromatosis type 1. *Am J Hum Genet* 81:243–251. <https://doi.org/10.1086/519562>
- Messiaen L, Yao S, Brems H et al (2009) Clinical and mutational spectrum of neurofibromatosis type 1-like syndrome. *JAMA* 302:2111–2118. <https://doi.org/10.1001/jama.2009.1663>
- Messiaen LM, Callens T, Mortier G et al (2000) Exhaustive mutation analysis of the NF1 gene allows identification of 95% of mutations and reveals a high frequency of unusual splicing defects. *Hum Mutat* 15:541–555. [https://doi.org/10.1002/1098-1004\(200006\)15:6<3c541::AID-HUMU6%3e3.0.CO;2-N](https://doi.org/10.1002/1098-1004(200006)15:6<3c541::AID-HUMU6%3e3.0.CO;2-N)
- Minoche AE, Lundie B, Peters GB et al (2021) ClinSV: clinical grade structural and copy number variant detection from whole genome sequencing data. *Genome Med* 13:32. <https://doi.org/10.1186/s13073-021-00841-x>
- Pacot L, Vidaud D, Sabbagh A et al (2021) Severe phenotype in patients with large deletions of NF1. *Cancers (Basel)* 13:2963. <https://doi.org/10.3390/cancers13122963>
- Pasmant E, de Saint-Trivier A, Laurendeau I et al (2008) Characterization of a 7.6-Mb germline deletion encompassing the NF1 locus and about a hundred genes in an NF1 contiguous gene syndrome patient. *Eur J Hum Genet* 16:1459–1466. <https://doi.org/10.1038/ejhg.2008.134>
- Pasmant E, Parfait B, Luscan A et al (2015) Neurofibromatosis type 1 molecular diagnosis: what can NGS do for you when you have a large gene with loss of function mutations? *Eur J Hum Genet* 23:596–601. <https://doi.org/10.1038/ejhg.2014.145>
- Pasmant E, Sabbagh A, Hanna N et al (2009a) SPRED1 germline mutations caused a neurofibromatosis type 1 overlapping phenotype. *J Med Genet* 46:425–430. <https://doi.org/10.1136/jmg.2008.065243>
- Pasmant E, Sabbagh A, Masliah-Planchon J et al (2009b) Detection and characterization of NF1 microdeletions by custom high resolution array CGH. *J Mol Diagn* 11:524–529. <https://doi.org/10.2353/jmoldx.2009.090064>
- Pasmant E, Vidaud M, Vidaud D, Wolkenstein P (2012) Neurofibromatosis type 1: from genotype to phenotype. *J Med Genet* 49:483–489. <https://doi.org/10.1136/jmedgenet-2012-100978>
- Perez-Becerril C, Evans DG, Smith MJ (2021) Pathogenic noncoding variants in the neurofibromatosis and schwannomatosis predisposition genes. *Hum Mutat* 42:1187–1207. <https://doi.org/10.1002/humu.24261>
- Leman R, Parfait B, Vidaud D et al (2022) SPiP, a comprehensive splicing prediction pipeline for massive detection of exonic and intronic variant effect on mRNA splicing. *Hum Mutat*. <https://doi.org/10.22541/au.164544915.57104749/v1>
- Ratner N, Miller SJ (2015) A RASopathy gene commonly mutated in cancer: the neurofibromatosis type 1 tumour suppressor. *Nat Rev Cancer* 15:290–301. <https://doi.org/10.1038/nrc3911>
- Rentzsch P, Schubach M, Shendure J, Kircher M (2021) CADD-Splice—improving genome-wide variant effect prediction using deep learning-derived splice scores. *Genome Med* 13:31. <https://doi.org/10.1186/s13073-021-00835-9>
- Richards S, Aziz N, Bale S et al (2015) Standards and guidelines for the interpretation of sequence variants: a joint consensus recommendation of the American College of Medical Genetics and Genomics and the Association for Molecular Pathology. *Genet Med* 17:405–424. <https://doi.org/10.1038/gim.2015.30>
- Robinson JT, Thorvaldsdóttir H, Winckler W et al (2011) Integrative genomics viewer. *Nat Biotechnol* 29:24–26. <https://doi.org/10.1038/nbt.1754>
- Sabbagh A, Pasmant E, Imbard A et al (2013) NF1 molecular characterization and neurofibromatosis type I genotype-phenotype correlation: the French experience. *Hum Mutat* 34:1510–1518. <https://doi.org/10.1002/humu.22392>
- Salomon LJ, Sotiriadis A, Wulff CB et al (2019) Risk of miscarriage following amniocentesis or chorionic villus sampling: systematic review of literature and updated meta-analysis. *Ultrasound Obstet Gynecol* 54:442–451. <https://doi.org/10.1002/uog.20353>
- Trost B, Walker S, Wang Z et al (2018) A comprehensive workflow for read depth-based identification of copy-number variation from whole-genome sequence data. *Am J Hum Genet* 102:142–155. <https://doi.org/10.1016/j.ajhg.2017.12.007>
- Yasunari T, Shiraki K, Hattori H, Miki T (2000) Frequency of choroidal abnormalities in neurofibromatosis type I. *Lancet* 356:988–992. [https://doi.org/10.1016/S0140-6736\(00\)02716-1](https://doi.org/10.1016/S0140-6736(00)02716-1)
- Yeo G, Burge CB (2004) Maximum entropy modeling of short sequence motifs with applications to RNA splicing signals. *J Comput Biol* 11:377–394. <https://doi.org/10.1089/1066527041410418>

Publisher's Note Springer Nature remains neutral with regard to jurisdictional claims in published maps and institutional affiliations.

Springer Nature or its licensor holds exclusive rights to this article under a publishing agreement with the author(s) or other rightsholder(s); author self-archiving of the accepted manuscript version of this article is solely governed by the terms of such publishing agreement and applicable law.